$(LiH_2)^+$ energy surface and Li^+ on D_2 scattering

A. Russek, R. Snyder, and R. J. Furlan
Department of Physics, The University of Connecticut, Storrs, Connecticut 06269
(Received 12 December 1988)

Recent measurements of vibrorotational excitation in low-keV-energy $Li^+ + D_2$ collisions have shown a breakdown in a rather general scaling law for projectile energy loss in the quasielastic channel. This scaling law maintains that in small-angle impulsive scattering determined by a conservative potential, classical trajectory calculations of atomic projectiles on diatomic targets predict a universal scaled vibrorotational excitation energy spectrum when $Q/E\theta^2$ is plotted as a function of $\tau = E\theta$. The breakdown in scaling is here shown to be caused by quantization of vibrational energy in the target molecule. It is also shown that the critical angle at which departure from purely elastic scattering occurs is given by $E\theta_c^2 = \text{const}$. The theory predicts that in the collision-energy regime of 500 eV to a few keV and for scattering angles in excess of a few tenths of a degree, the vibrorotational excitation energy in D_2 is almost entirely vibrational, with only a small fraction of the excitation energy going into rotational degrees of freedom.

I. INTRODUCTION

Any attempt to make progress toward an *ab initio* understanding of chemical processes begins with a knowledge of the energy surface. It was first pointed out by Ioup and Russek[1] that an experimental investigation of the energy surface of a triatomic molecular system could be more effectively carried out with atom-on-molecule collisions in a higher collision-energy range than that in which chemical rearrangements take place. In the collision energy range from a few hundred eV to a few keV, the collisions are sufficiently *slow* so that they are probing the same adiabatic energy surface that is also responsible for chemical reactions. At the same time, the collisions are sufficiently *fast* to enable the nuclear motion (including rotational and vibrational excitation of the molecular targets) to be treated both classically and impulsively[2] when attempting to unfold the energy surface from the scattering data. For a study of the adiabatic energy surface, only the electronic state need adjust adiabatically to the changing internuclear separation. The occurrence of vibrorotational excitation in these collisions does not make the theoretical interpretation more difficult. Quite to the contrary, several recent papers[3-6] have demonstrated that differential projectile energy-loss measurements in quasielastic collisions of atoms or ions with diatomic molecules in the low-keV-energy range constitute a sensitive probe of the ground-state energy surface of the triatomic molecular system. Quasielastic collisions are those which are elastic insofar as the electronic motion is concerned, following the adiabatic or diabatic energy surface, but which may be inelastic with respect to the rotational and vibrational degrees of freedom. Vibrorotational excitation induced in the molecular target by the projectile atom actually yields more detailed information on the energy surface of the triatomic molecule, provided that doubly differential energy-loss measurements (differential in both energy loss and angle) are taken at collision energies such that the nuclear motion can be treated impulsively. This is the collision-energy range of a few hundred eV to a few keV. Below this energy range even the nuclear motion becomes adiabatic (at about 50 eV), and very little can be learned without solving thousands of close-coupled scattering equations involving the energetically accessible rotational and vibrational states. At the other end of the collision-energy range, above a few keV, one can no longer be certain that the electronic motion is evolving along the adiabatic energy surface.

For those collision systems in which there are no surface intersections between the ground-state energy surface and those of excited electronic states, Sigmund[7,8] has proven that for small-angle collisions, the scaled projectile energy loss $\Delta E/E\theta^2$ is a function of $\tau = E\theta$ only, where E and θ are the projectile energy and scattering angle. Such a scaling law is of considerable importance; if it is obeyed, it conclusively demonstrates that the scattering forces are derived from a velocity independent potential, and that the electronic motion is adiabatically (or diabatically) adjusting to the changing internuclear separation. The converse, however, is not true. Sigmund scaling can break down for a variety of reasons, so that a breakdown of scaling does not necessarily imply a breakdown of adiabatic behavior.[9] Indeed, one of the main results of this work is the explanation of just such a case.

The Sigmund scaling law was confirmed[3,4] in the Ne^+ on D_2 and Ne on D_2 systems, for which electronically inelastic channels were known to be weak. It was also confirmed[6] for quasielastic collisions in the He on D_2 system, which has strong electronic excitation channels, despite the fact that these collisions violate one of the assumptions under which the scaling law was derived. Even where electronic excitation can occur, if one observes only the electronically elastic channels, the experiments probe the adiabatic or diabatic surface. It was also established, both experimentally[3,4,6] and theoretically,[10,5]

that for all the projectiles mentioned above, Ne, Ne^+, and He, the H_2 covalent bond is the principal scattering agent in the energy range up to at least a few keV. The molecular energy for the triatomic molecular system can be written as the sum of the energy describing an isolated H_2 plus an interaction term due to the proximity of the third component. In terms of the variables R, r, and γ describing the molecular geometry (see Fig. 1),

$$V(R,r,\gamma)=V_{H_2}(r)+E(Li^+)+V_{int}(R,r,\gamma)\ . \tag{1}$$

Because the physics of molecules is very rich, a parametric description of V_{int} is, of necessity, quite complicated. However, in the regime of collision energy and scattering angle of interest in this work, only two terms dominate: a pair of screened Coulomb potentials describing the electrostatic repulsion between the projectile (of nuclear charge Z) and each of the protons, plus an interaction, $V_{cb}(R)$, between the projectile and the covalent bond:

$$V_{int}(R,r,\gamma)\cong Z\left[\frac{e^{-\lambda_c R_A}}{R_A}+\frac{e^{-\lambda_c R_B}}{R_B}\right]+V_{cb}(R)\ . \tag{2}$$

The covalent bond is a quantum mechanical effect which draws the two hydrogen electrons into the region between the two protons, centered on the midpoint between the two ($R=0$) and roughly spherical about the H_2 center. As a consequence, the potential generated by the covalent bond is a function of R only. Such a potential can deflect the projectile, but it cannot induce vibrorotational excitation in the H_2 target, since it does not involve the internal coordinates of the latter. On the other hand, the electrostatic repulsion term of (2) does involve the internal coordinates r and γ via R_A and R_B, and is able to excite the vibrorotational degrees of freedom of the molecular target. It was shown in Snyder and Russek[5] that insofar as projectile energy loss is concerned, this screened Coulomb term leads to a collision process very close to the binary limit, a limit wherein half of the projectile energy loss goes into vibrorotational excitation and half goes into recoil energy of the target molecule center of mass.

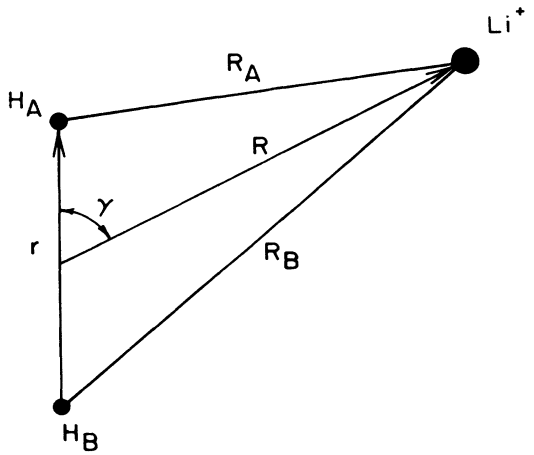

FIG. 1. Triatomic molecular geometry.

The observed behavior in the differential projectile energy-loss measurements for the collision systems depends on the interplay between these two terms in V_{int}. For noble gas projectiles, the screened Coulomb core-core terms are short range by comparison with the covalent bond contribution. Thus, V_{cb} prevails at large values of R; it is repulsive, and is rather well approximated by a Born-Mayer term: $A_3 e^{-\lambda_p R}$. The strength is denoted by A_3, because V_{cb} is a three-body contribution to the adiabatic molecular energy surface. When, during the collision process, the noble gas atom is near the covalent bond, the electron distribution of the atom overlaps that of the covalent bond, forcing too many electrons into the same spatial volume. Antisymmetrization of the electron wave function raises this overlapping portion to higher energy states, thereby raising the overall electronic energy. The greater the overlap, the higher the overall electronic energy. Thus, the interaction between a noble gas atom and the covalent bond is a repulsive potential. This description is a heuristic account of what is actually seen in *ab initio* calculations of the molecular energy surface.[10] These *ab initio* calculations show V_{cb} to be very close to a Born-Mayer potential. For noble gas atoms, the covalent bond contribution dominates at large R, because the screened Coulomb core-core terms are short range. Consequently, collisions with a large impact parameter (small values of $\tau=E\theta$) will be completely elastic, because $V_{cb}(R)$ is unable to vibrotationally excite the target H_2. As impact parameters decrease, τ increases, but the collisions remain completely elastic until τ reaches the maximum value that can be produced by the Born-Mayer term V_{cb}.[11] Values of τ larger than this critical value can only be achieved by the core-core terms, when the projectile penetrates the covalent bond and interacts with the cores of the target molecule. These two-body core-core interactions produce considerable vibrational excitation along with projectile scattering. At the critical value of τ, therefore, vibrational excitation energy, Q, changes abruptly from zero to a substantial fraction of the target recoil energy. This critical value of τ is here referred to as the "breakaway point." It must again be stressed that the physical picture drawn above is not an assumption, it is a simplified account of what is actually obtained in classical trajectory scattering calculations using the *ab initio* molecular potential.

This paper concerns the $(LiH_2)^+$ energy surface and Li^+ on D_2 scattering. Insofar as the energy surface is concerned $(LiD_2)^+$ and $(LiH_2)^+$ are identical, so that the experiments,[12,13] on D_2 probe the $(LiH_2)^+$ energy surface. The use of D_2 as a target molecule in the experiments is for calibration purposes;[13] with D_2 targets, the projectile energy loss for zero vibrorotational excitation energy can be calibrated against projectile energy loss with He targets.

The collision system Li^+ on D_2 is isoelectronic with the neutral collision system He on D_2, but does not have the strong electronic excitation channels of the latter in the keV collision-energy range. Thus, Li^+ on D_2 collisions satisfy the conditions for Sigmund scaling. However, the experimental results show a surprising break-

down in Sigmund scaling for Li^+ on D_2, whereas He on D_2 obeys the scaling law despite the presence of strong electronic excitation channels. This breakdown in Sigmund scaling for Li^+ on D_2 is shown in Sec. III to be a quantum effect, which occurs because the breakaway from the elastic scattering limit falls in a region of low excitation energy. The D_2 molecular target can only be vibrationally excited in discrete quanta $\hbar\omega_c$; at the same time, rotational excitation is very weak. The scaling breakdown can be entirely accounted for by incorporating into the classical scattering calculations the ansatz that all collisions for which the classically calculated excitation energy $Q<\frac{1}{2}\hbar\omega_c$ is registered as $Q=0$; all collisions for which $\frac{1}{2}\hbar\omega_c<Q<\frac{3}{2}\hbar\omega_c$ is registered as $Q=1\hbar\omega_c$, and so forth.

The question arises: why was this effect not observed previously? The answer is to be found in the difference between Li^+ and a noble gas. For all collision systems, the covalent bond contribution to the scattering potential keeps the projectile outside the range of the screened Coulomb two-body potential for the gentler collisions (small τ), yielding perfectly elastic collisions $Q=0$. For noble gas projectiles, the screened Coulomb core-core terms are short range, but for Li^+ projectiles, the ranges of these core-core terms are considerably longer, almost as long as the range of the covalent bond term itself. Because of this, a Li^+ projectile can penetrate into the range of the screened Coulomb core for much gentler collisions than can noble gas projectiles, with correspondingly smaller excitation energies. Indeed, for Li^+ on D_2, a substantial percentage of the classically computed excitation energies are smaller than $\frac{1}{2}\hbar\omega_c=0.18$ eV, thereby making vibrational quantization a significant factor to be taken into account. It was anticipated in Heckman *et al.*[12] that the breakaway from the elastic limit would scale as $E\theta^2$, a prediction that has been borne out by the classical trajectory calculations reported in this paper which are based on an *ab initio* $(LiH_2)^+$ molecular energy surface.

II. THEORY

A. Review of scaling theory

Sigmund[7,8] first suggested that, under rather general conditions which should be valid in the keV collision energy regime, both the projectile energy loss, ΔE, and the vibrorotational excitation energy, Q, scaled in units of $(M_P/M_T)E\theta^2$, are functions of τ only: they do not depend separately on the collision energy. Here, M_P is the projectile mass, and M_T is the total mass of the molecular target. The quantity $(M_P/M_T)E\theta^2$ is the recoil kinetic energy of translational motion of the target molecule in small-angle impulsive scattering: it is also the energy that would be lost by the projectile in a completely elastic collision:

$$\Delta E_{\rm el}=P^2/2M_T=\frac{M_P}{M_T}E\theta^2 . \tag{3}$$

In mathematical terms, the Sigmund scaling law states that the dimensionless ratios, q and f, defined by

$$Q/\Delta E_{\rm el}=q(\tau) , \tag{4}$$

$$\Delta E/\Delta E_{\rm el}=2f(\tau) , \tag{5}$$

are functions of $\tau=E\theta$ only. The factor of 2 on the right-hand side of Eq. (5) has been incorporated to retain the original Sigmund definition of f. Here, E and θ are the projectile energy and scattering angle, and P is the recoil momentum of the center of mass of the target molecule, all in the laboratory frame of reference. Since conservation of energy requires that $\Delta E=Q+\Delta E_{\rm el}$, q and f are related by $2f=q+1$.

Sigmund rigorously derived the scaling law Eqs. (3)–(5) provided that (i) nuclear motion can be described in terms of classical trajectory calculations, (ii) the impulse approximation is valid, (iii) small-angle scattering approximations hold, and (iv) the forces are derivable from a potential that is *velocity independent.* The derivation permits the electronic motion to be treated quantum mechanically, with the adiabatic or diabatic electronic energy incorporated in the conserved potential $V(R,r,\gamma)$ used in the classical trajectory calculations. The derivation does not require this potential to have any particular form. However, if V can be expressed as a combination of Bohr and Born-Mayer potentials, it was shown by Snyder and Russek[5] that in the impulse approximation the quantities $q(\tau)$ and $f(\tau)$ can be obtained in closed form for each collision geometry (i.e., a given impact parameter and a given orientation of the target molecule). Since the classical trajectory calculations must be performed for about 10^5 collision geometries to obtain a reasonably accurate doubly differential cross section, the closed form solution for the momentum transfer due to each component $V_{\rm int}$ is necessary to make the calculation tractable. In this work, the set of potentials with closed form solutions was extended to include potentials of the form

$$V_{\rm pol}=-C_p\left[\frac{1}{R_A^4+a^4}+\frac{1}{R_B^4+a^4}\right] . \tag{6}$$

With the procedure formulated in Ref. 5, it is necessary to know the momentum transfer between the projectile and each of the nuclei. For a potential term of the form $V=-C_p/(r^4+a^4)$, where r stands for R_A or R_B, the momentum transfer, P, is given by

$$P=-\frac{C_p\pi b(u+2b^2)(u-b^2)^{1/2}}{va^2u^2\sqrt{2}} , \tag{7}$$

where v is the collision velocity, b the impact parameter to the center under consideration, and $u=(a^4+b^4)^{1/2}$. The vectors P_A and P_B lie along R_A and R_B and are attractive impulses.

B. Quantization of vibrational excitation

The vibrational states of D_2 are separated by approximately 0.35 eV. Vibrational quantization is easily taken into account in a classical trajectory treatment by replac-

ing the calculated excitation energy of the D_2 target by multiples of this energy quantum. The classically calculated excitation energy represents the mean of a *distribution* of excitation energies that would follow from a proper quantum mechanical treatment. Hence, if, for a given collision geometry, the classically calculated excitation energy is evaluated to be slightly less than $\hbar\omega_c$, a correct quantum mechanical calculation would hold that the molecule would acquire a full quantum of excitation energy for slightly less than half of the collisions with that collision geometry. Thus, quantization of the classical trajectory treatment is implemented by dividing the excitation energy scale according to the ansatz: all collision geometries for which the classically calculated excitation energy lies in the range

$$(n-\tfrac{1}{2})\hbar\omega_c \le Q \le (n+\tfrac{1}{2})\hbar\omega_c$$

are recorded as $Q=n\hbar\omega_c$. All collisions for which $0\le Q\le \frac{1}{2}\hbar\omega_c$ are recorded as elastic scattering, $Q=0$.

For this vibrational quantization of classical trajectory calculations to be valid, rotational excitation must not be a significant factor, and it is not. In the worst case of a completely binary collision between the projectile and a single D, with momentum transfer at right angles to the D-D axis, then all the excitation energy would go into rotational motion. However, Figs. 4(a) and 4(b) show the excitation process to be only 30% binary. (A completely binary collision would give $q=1$.) Moreover, even statistically, only half the binary collisions would be so oriented as to make the excitation primarily rotational. In fact, the orientations are not statistical. The impact geometries, which dominate the region of breakaway from the elastic limit, are such as to yield small angular momentum transfer.

C. The interaction potential

The interaction energy, $V_{\rm int}(R,r,\gamma)$, between $Li^+(^1S)$ and $H_2(X\,^1\Sigma_g^+)$ has been determined with single configuration SCF calculations of the $Li^+ + H_2$ energy surface. The energy surface is denoted by $V(R,r,\gamma)$ in Eq. (1). The basis set used for Li^+ was a set of Gaussian functions suggested by Lester[14,15] and similar to that used by Kutzelnigg *et al.*[16] It consists of nine *s*-type Gaussians from the atomic basis set for Li^+ by Huzinaga,[17] with the first four Gaussians contracted to a single *s*-type function and the remaining five uncontracted, together with three *p*-type functions to describe polarization. The H_2 basis set is the same as that used by Russek and Garcia,[10] derived from Brown and Hayes.[18] Centered on each H are five *s*-type Gaussians, with the first two contracted, and two *p*-type Gaussians. A sample of the results of the *ab initio* calculation are shown as circles and crosses in Fig. 2; the curves illustrate the quality of a parametric fit of a form suggested in Russek and Garcia, slightly modified to account for the ionic nature of Li^+.

Calculations were carried out for H-H separations $r=1.0$, 1.4, and 1.8 a.u., the full angular range, $\gamma=0°$, 30°, 60°, and 90°, and R ranging from 0 to 10 a.u. The parametric form to which the *ab initio* calculations were

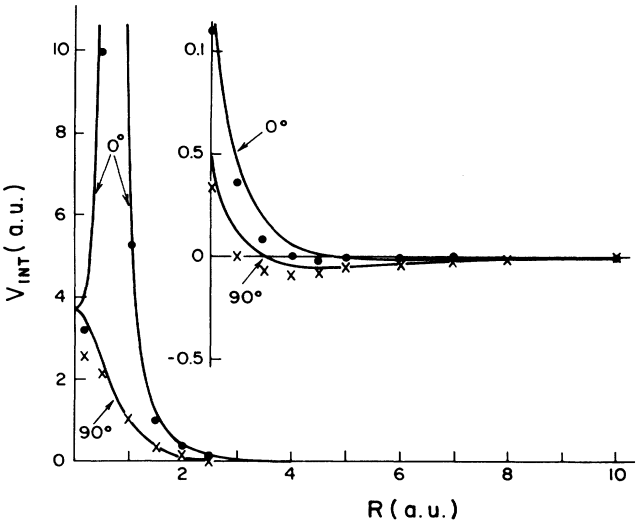

FIG. 2. Representative sample of the *ab initio* calculations for $V_{\rm int}$ and the fit of the parametric form given by Eqs. (6) and (8)–(10). The circles give the *ab initio* calculated values at $\gamma=0°$, the crosses give the calculated values at $\gamma=90°$, the curves give the best fit to the *ab initio* calculated values, obtained with the values for the parameters given in the text.

fit is of the form

$$V_{\rm int}=V_{\rm pol}+V_{\rm Coul}+V_{\rm BM}\ . \tag{8}$$

It consists of a saturated dipole polarization term, a Coulomb term and a Born-Mayer term. The polarization term is given by Eq. (6), with $C_p=1.7$ and $a=4.0$. It does not make any significant contribution in the range of collision energies and scattering angles under consideration; it is included for completeness only. The remaining two terms of (8) are given by

$$V_{\rm Coul}=(Z-\tfrac{1}{2}Z_b)\left[\frac{e^{-\lambda_c R_A}}{R_A}+\frac{e^{-\lambda_c R_B}}{R_B}\right] +Z_b\left[\frac{0.5}{R_A}+\frac{0.5}{R_B}-\frac{(1-e^{-R/r_b})}{R}\right] \tag{9}$$

and

$$V_{\rm BM}=A_3\left[e^{-\lambda_p R}-\frac{1}{\beta}e^{-\beta\lambda_p R}\right]\ . \tag{10}$$

Of the constants which appear in Eqs. (9) and (10), Z represents the product of the Li and H nuclear charges, and was fixed at 3. The remaining constants were fit to the *ab initio* calculations, yielding $Z_b=0.81$, $\lambda_c=1.8$, $\lambda_p=1.67$, $\beta=2.6$, and $r_b=0.75$. The parameter Z_b describes the amount of charge drawn into the H_2 covalent bond and centered at the H-H midpoint, $R=0$; the parameters β and r_b relate to the diffuseness of the covalent bond charge distribution. Even though the H_2 is at its equilibrium separation of 1.4, the parametric form was fit to the calculated values at $r=1.0$, 1.4, and 1.8, because

vibrational excitation depends on $\partial V_{\text{int}}/\partial r$. With three H-H separations and four angles for each separation, 12 curves were checked against the *ab initio* calculations. The curves shown in Fig. 2 are representative of the accuracy of the fit. Most of the discrepancies arise from the insistence on expressing V in terms of Bohr, Born-Mayer, and cutoff polarization potentials, for which the momentum transfer in the impulse approximation is known in closed form. In particular, the largest discrepancy, at $R=0.2$, is a consequence of using the form given by (10) for V_{BM} and adjusting the constants to give a good fit for values of $R \geq 0.5$. The region inside $R=0.5$ could be corrected by an additional short-range Born-Mayer term. It was not done, however, because the small region near the origin does not make a substantial contribution to the energy-loss distributions.

III. RESULTS AND COMPARISON WITH EXPERIMENT

The details of the classical trajectory computation methods have been described in Ref. 5 and will only briefly be summarized here. A straight line trajectory is used with given impact parameter and initial H-H orientation. Each set of three initial conditions is here referred to as a "collision geometry," and for each, the scattering angle θ, recoil energy of the H_2 center of mass ΔE_{el}, and vibrorotational excitation energy Q, are all calculated in the impulse approximation. In this method, the *ab initio* calculated $V_{\text{int}}(R,r,\gamma)$ must be approximated as a sum of two center potentials between the projectile and three specified points in the H_2 target: the two protons (or deuterons) and the center of the covalent bond, $R=0$. Momentum transfers, $\mathbf{P}_i$, are determined for each center, and these are then analyzed to obtain θ, ΔE_{el}, and Q. The quantities θ and ΔE_{el} follow from the total momentum transfer, $\mathbf{P}_T=\sum_i \mathbf{P}_i$, while Q is determined by the momentum transfer *relative* to the H_2 center of mass. To make the problem tractable, it is essential that for each individual two-body potential in the approximation to V_{int}, the momentum transfer in the impulse approximation be known in closed form. Because approximately 10^5 collision geometries are required for the necessary resolution in the distribution in Q associated with each scattering angle θ, computing time would be prohibitive if the Newtonian equations of motion had to be integrated for each collision geometry.

Figure 3 shows one typical outcome of these calculations. It is the spectrum of target excitation energies obtained when $E=1$ keV and $\tau=2.0$ keV deg. It shows that the most probable event is excitation to the third vibrational level, with a corresponding $q=0.32$, where q is scaled vibrational excitation energy defined by Eq. (4). Similar calculations at other scattering angles lead to the results shown in Fig. 4, which shows the dependence of the most probable q, denoted by q_m, as a function of τ. The qualitative features of the dependence are intuitively plausible: small scattering angles are, of course, dominated by purely elastic scattering, $q_m=0$. At some larger scattering angle, excitation to the second vibrational state becomes most probable, with a corresponding jump in q_m. This second vibrational state remains dominant for some range of τ, during which q_m falls off parabolically according to Eq. (4), since Q stays constant, while ΔE_{el} increases with increasing τ. When τ increases to the point where the third state becomes most probable, a second jump occurs in q_m, and so forth, as successively higher vibrational states become dominant.

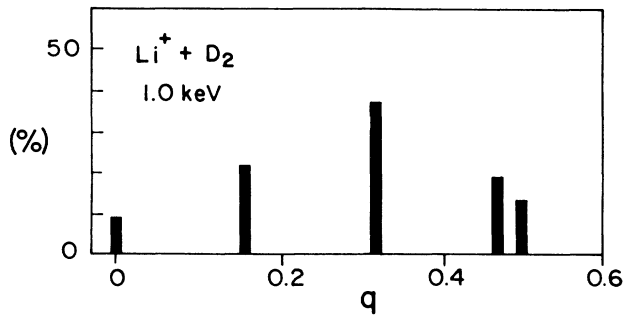

FIG. 3. Typical spectrum of scaled molecular excitation energies q. This spectrum is for $E=1$ keV, $\tau=2$ keV deg, and shows a most probable q value of 0.32, corresponding to the third vibrational level.

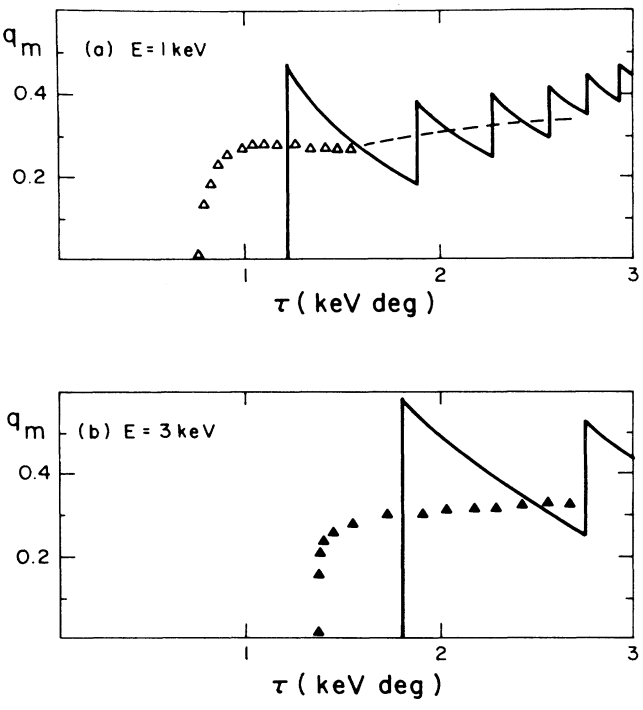

FIG. 4. Most-probable reduced excitation q_m vs τ at projectile energies (a) 1 keV and (b) 3 keV. The solid line gives the theoretical prediction from the quantized model described in Sec. II of this work. The triangles give the experimental data from Heckman and Pollack (Ref. 13). Because the 1 keV data was limited to $\tau \leq 1.5$ keV deg, the dashed line shows the common trend followed by all the experimental data for $\tau \geq 1.5$ keV deg. In this region, Sigmund scaling is obeyed, so q_m can be obtained from the results at higher energies.

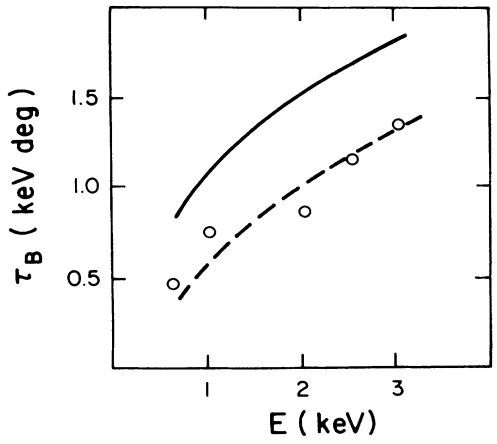

FIG. 5. Breakaway τ values vs projectile energy, E. The solid line gives the theoretical predictions, the circles give the experimental values from Heckman and Pollack (Ref. 13). The dashed line is a smooth fit through the experimental points.

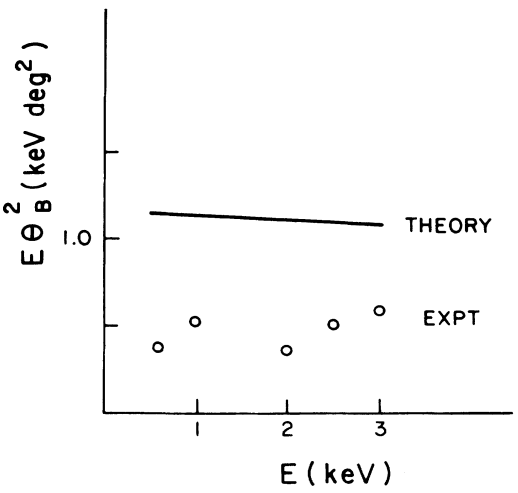

FIG. 6. Values of $E\theta^2=\tau^2/E$ at which the breakaway occurs, plotted as a function of E. The solid line gives the theoretical predictions, the circles give the experimental values.

Figure 4 also shows experimental results of q values from Heckman and Pollack,[13] which were taken with a finite angular resolution ($\simeq 0.1°$ FWHM) and also averaged over small angular ranges. As a consequence, the experimental data points are unable to resolve the predicted sawtooth structure, but they are seen to lie midway between the peaks and valleys predicted by the quantized classical trajectory calculations. In addition, some smoothing results from rotational excitation, which although small, is not entirely absent. At small values of τ, the theory and experiment agree in showing a very abrupt rise in q_m at a breakaway value of τ which depends on the projectile energy. In Fig. 5, this breakaway value of τ is plotted as a function of E, for both theory and experiment. The figure shows that the theoretical and the experimental curves have the same functional dependence, with the theory offset some 0.5 keV deg higher, confirming that the breakdown of Sigmund scaling in this collision system is due to quantization of the vibrational excitation of the molecular target. Finally, Fig. 6 shows the same results as Fig. 5, but with $E\theta^2$, rather than τ, plotted as a function of E. It is clear from this figure that the breakaway from elastic scattering scales as $E\theta^2$, as was predicted by Heckman *et al.*[12] Denoting by θ_c the critical angle at which the breakaway from elastic scattering occurs, Fig. 6 shows that the theory predicts $E\theta_c^2=1.2$ keV deg^2, while the experimental value is 0.5 keV deg^2. The cause of this systematic discrepancy most likely lies in the experimental determination of the "most probable q value" from the bimodal distribution that the theory predicts in the vicinity of the breakaway point. In the theory, this is the highest point in the distribution in q. With insufficient experimental resolution (0.5 eV per 1000 eV) to resolve individual vibrational peaks and with statistical fluctuations in the spectra, the experimental q_m was determined from the *mean* value of the upper half of the spectral distribution. Such a method of locating the peak is valid over most of the τ range and would be fine for a simple Gaussian distribution, but would cause a systematic reduction in the τ value for the breakaway. This critical value of τ is the one for which the fraction of targets left in the first excited state equals the fraction left in the ground vibrational state. Below that value of τ where, say 60% of the targets are in the ground state, 36% in the first excited vibrational state, and 4% in the second excited vibrational state, the computer locates q_m at $q=0$. For this same value of τ, the experimental determination would locate q_m midway between $q=0$ and that value of q corresponding to the first excited state (i.e., beyond the elastic limit). Clearly, this measurement tends to locate the breakaway at lower values of τ than that given by the theoretical prediction. In this connection, it is noted that some data set distribution in Fig. 4 of the preceding paper showed elastic peaks at values of τ consistent with the theoretical prediction.

ACKNOWLEDGMENTS

This work was supported by the National Science Foundation under Grant No. PHY-8507736.

[1]J. Ioup and A. Russek, Phys. Rev. A **8**, 2898 (1973).
[2]A. Russek, *Electronic and Atomic Collisions,* edited by J. Eichler, I. V. Hertel and N. Stolterfoht (Elsevier, New York, 1984), p. 701.
[3]N. Andersen, M. Vedder, A. Russek, and E. Pollack, J. Phys. B **11**, L493 (1978).
[4]N. Andersen, M. Vedder, A. Russek, and E. Pollack, Phys. Rev. A **21**, 782 (1980).
[5]R. Snyder and A. Russek, Phys. Rev. A **26**, 1931 (1982).
[6]J. Jakacky, Jr., E. Pollack, R. Snyder, and A. Russek, Phys.

Rev. A **31**, 2149 (1985).
[7]P. Sigmund, J. Phys. B **11**, L145 (1978).
[8]P. Sigmund, J. Phys. B **14**, L321 (1981).
[9]R. Snyder and A. Russek, in *Abstracts of Papers, Proceedings of the Fourteenth International Conference on the Physics of Electronic and Atomic Collisions, Palo Alto, 1985,* edited by M. J. Coggiola, D. L. Huestis, and R. P. Saxon (North-Holland, Amsterdam, 1986), p. 560.
[10]A. Russek and R. Garcia, Phys. Rev. A **26**, 1924 (1982).
[11]R. Snyder and A. Russek, in *Abstracts of Papers, Proceedings of the Thirteenth International Conference on the Physics of Electronic and Atomic Collisions, Berlin, 1983,* edited by J. Eichler, W. Fristch, I. V. Hertel, N. Stolterfoht, and U. Wille (ICPEAC, Berlin, 1984), p. 597.
[12]V. Heckman, A. Russek, and E. Pollack, in *Abstracts of Papers, Proceedings of the Fifteenth International Conference on the Physics of Electronic and Atomic Collisions, Brighton, 1987,* edited by J. Geddes, H. B. Gilbody, A. E. Kingston, and C. J. Latimer (Queen's University, Belfast, 1987), p. 692.
[13]V. Heckman and E. Pollack, preceding paper, Phys. Rev. A **39**, 6154 (1989).
[14]W. A. Lester, Jr., J. Chem. Phys. **53**, 1511 (1970).
[15]W. A. Lester, Jr., J. Chem. Phys. **54**, 3171 (1971).
[16]W. Kutzelnigg, V. Staemmler, and C. Hoheisel, Chem. Phys. **1**, 27 (1973).
[17]S. Huzinaga, J. Chem. Phys. **42**, 1295 (1965).
[18]P. J. Brown and E. F. Hayes, J. Chem. Phys. **55**, 922 (1971).